

Braiding Intensity Analysis of a Post-Seismic Debris Flow Event Using a Comprehensive Indexing Tool

Rosdianah Ramli¹, Janice Lynn Ayog^{1,2,*}, Min Fui Tom Ngui^{1,3}, Rodeano Roslee^{2,4},
Felix Tongkul^{2,4}, Mohammad Radzif Taharin¹

¹Faculty of Engineering, Universiti Malaysia Sabah, Malaysia

²Natural Disaster Research Centre, Universiti Malaysia Sabah, Malaysia

³Eramaju Synergy Sdn Bhd, Lot 23, 2nd Floor Lido Plaza, Jalan Nosoob, 88300 Kota Kinabalu, Sabah, Malaysia

⁴Faculty of Science and Natural Resources, Universiti Malaysia Sabah, Malaysia

Received November 7, 2024; Revised February 17, 2025; Accepted April 17, 2025

Cite This Paper in the Following Citation Styles

(a): [1] Rosdianah Ramli, Janice Lynn Ayog, Min Fui Tom Ngui, Rodeano Roslee, Felix Tongkul, Mohammad Radzif Taharin, "Braiding Intensity Analysis of a Post-Seismic Debris Flow Event Using a Comprehensive Indexing Tool," *Environment and Ecology Research*, Vol. 13, No. 2, pp. 241 - 250, 2025. DOI: 10.13189/eer.2025.130205.

(b): Rosdianah Ramli, Janice Lynn Ayog, Min Fui Tom Ngui, Rodeano Roslee, Felix Tongkul, Mohammad Radzif Taharin (2025). *Braiding Intensity Analysis of a Post-Seismic Debris Flow Event Using a Comprehensive Indexing Tool*. *Environment and Ecology Research*, 13(2), 241 - 250. DOI: 10.13189/eer.2025.130205.

Copyright©2025 by authors, all rights reserved. Authors agree that this article remains permanently open access under the terms of the Creative Commons Attribution License 4.0 International License

Abstract River braiding occurs when sediment accumulates in a river section, resulting in bar formations that divide the flow into multiple channels, a phenomenon quantified as braiding intensity. This intensity is measured using a braiding index (BI), a metric essential for understanding sediment dynamics in braided rivers. While several braiding indices have been developed, many overlook key factors, such as the area occupied by bars, and often lack defined limits or unit-free properties, limiting their flexibility across diverse river types. Furthermore, conventional indices struggle to detect variations in braiding intensity in river reach sections with differing widths. Addressing these limitations, Das and Islam introduced a comprehensive, four-part braiding index tool that accommodates bar area, defined limits, and unit-free characteristics, enhancing its adaptability across various river conditions. However, this braiding index tool has not been applied for non-regulated, post-seismic flow events. Therefore, this study applies this novel braiding index tool to the Panataran river located in Sabah, Malaysian Borneo, a river significantly impacted by a 2015 post-seismic debris flow event, causing notable changes in its braiding river morphology. Using high-resolution satellite imagery, the study evaluates four distinct braiding indices— BI*, BI₁, BI₂ and BI₃—across six sections of the river, capturing both pre- and post-seismic debris flow conditions. Results reveal that the tool effectively quantifies changes in bar formation

and channel flow patterns, especially highlighting increased sediment deposition up to 42% in downstream sections. These findings hold practical implications for local stakeholders, including ecotourism operators and environmental authorities, providing essential data to identify erosion-prone areas or regions favourable for sustainable ecotourism development. By demonstrating the tool's ability to measure and monitor morphological changes in post-seismic river systems, this research underscores its broader utility in flood disaster response and vulnerability assessment, river management, and environmental planning, paving the way for future applications in other river systems affected by seismic events and similar geomorphological challenges.

Keywords Braided River, Braiding Index, Debris Flow, Mid-Channel Bars

1. Introduction

Rivers are amongst many natural forces shaping Earth's surface. The length and area of the world's rivers are estimated to be about 7.56 million km and 508,000km² respectively [1]. The morphological forms of river channels are the results of continuous active hydro-

geomorphic processes in their regions for the past several years. Rivers are a significant part of a dynamic fluvial system, and their characteristics can vary over time and space when exposed to various geomorphic factors. Geomorphic factors could be natural such as debris flow caused by post-seismic landslides coupled with heavy torrential rain [2, 3], or manmade such as land expansion for local tourism at riverbanks [4, 5]. Repeated exposures from such factors caused the river to adjust or modify in order to sustain its equilibrium state [6]. For example, several earthquakes that occurred in Central Sulawesi in 2018, which were also felt as far as the northern region of the Malaysian Borneo, had caused the rivers and floodplains in Jono-Oge to expand to accommodate massive sediment inflows triggered by post-seismic, large-scale flow-slides [7]. More recently, a post-seismic debris flow after an earthquake that happened in Mount Talamau, West Sumatra in 2022 caused slope instabilities with eroded materials from the upslope locations transported to the Bt. Timbo Abu River downstream, making the riverbed shallower [8].

In sustaining their equilibrium state, rivers often adjust their longitudinal slope and bed cross-sections, which are reflected in the rivers' channel patterns [9, 10]. Nimnate [10] added that the river's channel pattern is strongly affected by the sediment load (which may consist of either suspended and/or bed load) that is present in the river. Nimnate's [10] findings were affirmed by the observation made by Lalramchulloa et al. [11] in Tlawng river, concluding that when there is a gradual change in the sediment load, the river will adjust its longitudinal slope and/or bed cross-sections to accommodate such changes. Their observation thus relates the river's channel pattern with sediment transport processes, which are highly dependent on the sediment load and the river's transport capacity. These processes can be inferred from the formation and characteristics of river bars [12]. Several researchers [10, 13-15] have endeavoured to classify river's channel patterns (i.e. straight, meandering and braided) based on the sediment load and river's transport capacity. For straight rivers, the sediment load is usually lower than the transport capacity, resulting in stable riverbeds with minimal sediment deposition [12]. Meanwhile, meandering rivers are predominantly consisting of the suspended load, which are roughly balanced with the river's transport capacity. In contrast, braided rivers are dominated by bed loads that often exceed the transport capacity, leading to dynamic multi-channels formation with unstable bars and/or islands within the rivers.

Braided rivers are very sensitive to the increase of sediment load during extreme events such as flood and debris flow as these rivers tend to receive large sediment inflows but yield small sediment outflows [16-18]. By definition, braided river is a river characterised by bars

and/or islands formations that are formed by accumulation of sediment which then split the river into multiple channels and often with poorly defined banks [19, 20]. The degree of channel splitting within a river can be quantified as braiding intensity of the river or simply called as the braiding index [18]. Braiding index has been used to study and quantitatively analyse any changes in braided rivers [21]. Such assessment can be used in river management [22], infrastructure planning [23], and natural hazard prediction such as riverbank erosion [24].

Throughout the years, the braiding index has been developed based on three characteristics i.e. bar parameters (dimensions and frequency), number of channels, and the length of the channels in the river reach [25]. From these characteristics, four approaches have been used in existing braiding index which are (a) the length of bars per unit length of the reach [26], (b) the number of bars per unit length of the reach [27], (c) the length of channel links per unit length of the reach [28, 29], and (d) the number of channel links per cross-section [30, 31]. Das & Islam [32] have recently found that these classical braiding indexes do not consider the area occupied by bars, have no known limits and are not unit-free. They also found that by using any of these approaches, none could detect any variation in braiding intensity of reaches with same length and same bar parameters (number, length, and area), but with different channel widths. Therefore, they have developed a novel braiding index tool to enable comprehension of different braiding intensities for river reaches of different magnitudes of width. Nevertheless, this braiding index tool has only been used in regulated river [33-35] and studies are still lacking in using this tool to assess the impact of post-seismic debris flow on braided rivers.

Hence, this paper intends to assess the applicability of the braiding index tool developed by Das & Islam [32] to analyse the impact of a large-scale debris flow caused by an earthquake in the Malaysian Borneo, specifically on the braiding intensity of a river system close to the earthquake's epicentre. The paper is structured as follows: Section 2 describes the background of the study area including the debris flow event and its associated impacts. This section also discusses the data collated for the study along with the descriptions of the braiding index tool used. Section 3 discusses the key findings of the study, and finally, the conclusion of the study is presented in Section 4.

2. Materials and Methods

2.1. Background of Study Area

The study area (Figure 1) is located northeast of Kota Kinabalu, the state capital of Sabah, in the Malaysian Borneo. The nearest town is Kota Belud, situated at the downstream area of the Kadamaian river. The study area

focuses on one of the tributary rivers of Kadamaian called the Panataran river. The study area starts at the bailey bridge situated within the village of Melangkap (inset of Figure 1, black line) at the upstream of Panataran river to the river confluence linking to the Kadamaian river at the downstream. The total length of the Panataran river covered in this study is approximately 4.12 km with a mean bed slope of 3.2% that is considerably steep, and with an altitude between 160 m to 260 m above mean sea level.

The main source of flow for this river comes from the runoffs on the surfaces of Mount Kinabalu. The river catchment is largely enclosed by primary and secondary forests [36], and borders with a UNESCO World Heritage Site, the Kinabalu Global Geopark. The climate in the river basins is equatorial, with high temperatures (between 32.2 °C and 44.3 °C) and mean annual rainfall of approximately 2547.2 mm [37]. The area is predominantly influenced by the Northeast monsoon (November – March) with strong winds, and Southwest monsoon (late May – September) with lower humidity. Both monsoon seasons bring heavy rainfall and increase the river flow discharges, thus resulting in higher flood occurrences in villages residing along the riverbanks.

When a 6.0 Mw earthquake occurred on 5th June 2015 around Mount Kinabalu [38], the river systems located close to the epicentre were significantly affected; this included the Panataran river. Extensive rockfalls and landslides incidence around Mount Kinabalu, caused by the main shock and aftershocks, have provided abundant source materials for debris flow occurrence [39]. It was also reported that the deposition of large amounts of sediment loads, consisting of mud and loose boulders, happened along the river channels, which were then combined with heavy monsoonal rainfalls to trigger the

debris flows [40]. There were two separate debris flows events reported, however the one that happened in August 2015 significantly overloaded the Kadamaian river system that includes Panataran river with massive amount of sediment loads [41]. A study conducted by Chai et al. [37] found that amongst all the rivers around Mount Kinabalu, the Panataran river systems had the highest increase in river bars formation of 54.36 ha after the debris flow event. A spatial shift in the river was found 5 years after the debris flow event where 70% of the formed river bars changed back to other land covers such as vegetation, barren land, and river water while 30% of the formed river bars were preserved. In the same period (5 years after the debris flow event), it was found that 17.10 ha of river bars formed in the Panataran river. These changes implied that bed load mobilization is still active even after the post-seismic debris flow event and thus shows that the channel pattern particularly the braiding magnitude of Panataran river is continuously evolving. The existence of river bars, especially in the Panataran river, comes with unexpected benefits to the community as the bars have improved the river's aesthetic view, leading to the establishments of eco-tourism industries along the riverbanks [42]. An aerial photo showing the locations of eco-tourism industries in Melangkap village along the banks of Panataran river is shown in Figure 2. While this benefits the local community, the establishment of eco-tourism activities such as riverside camping and hostels may increase the flood vulnerability of the local communities as they may be unaware of the significant changes that happened on the channel pattern of the Panataran river. For example, on 23rd December 2022, 25 campers were rescued after being trapped by flood in one of Melangkap campsites along the river [43].

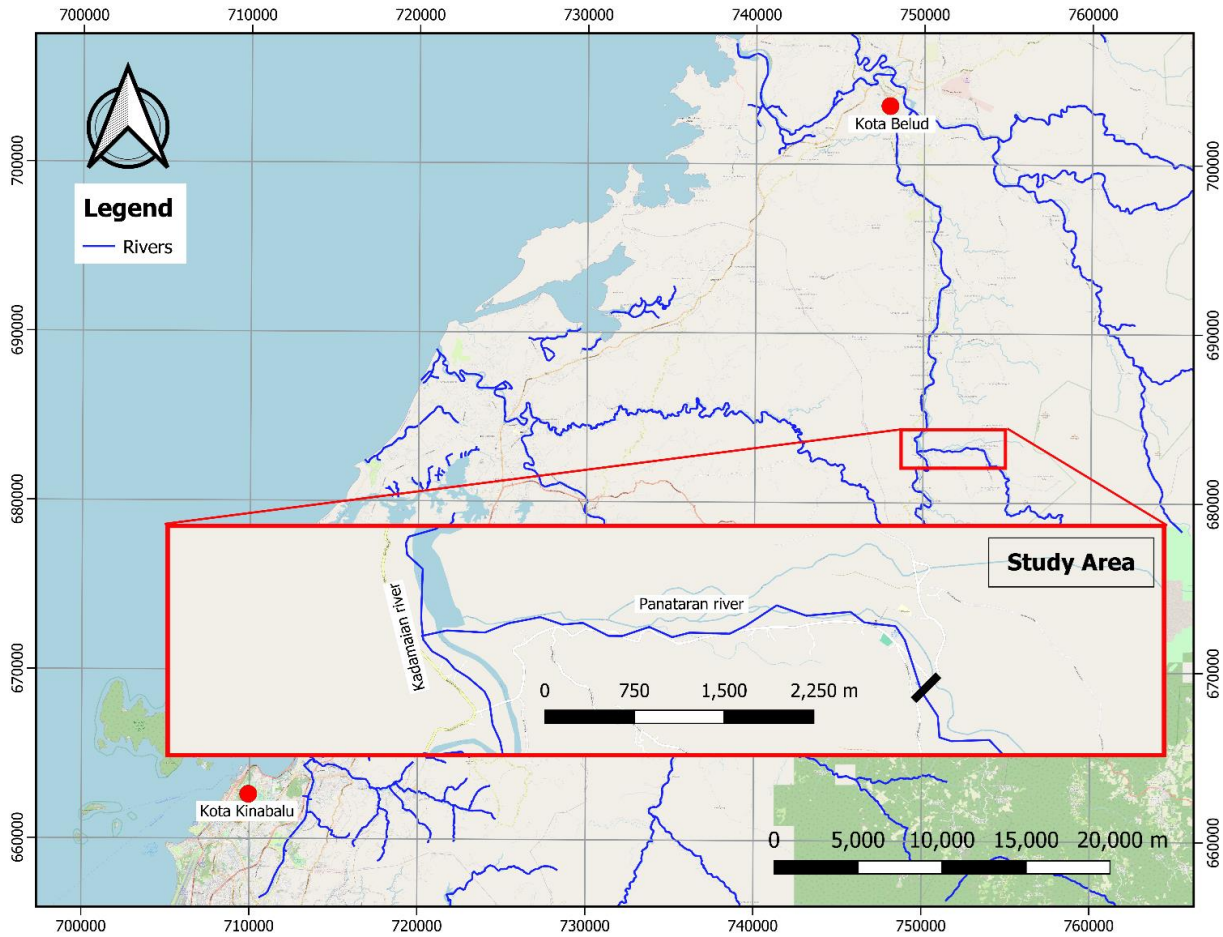


Figure 1. Location of the study area (red box) relative to Kota Kinabalu city and Kota Belud town, Sabah, Malaysia. The inset shows the zoomed-in image of the Panataran river and the location of the bailey bridge (thick black line) upstream of the river



Figure 2. Eco-tourism activities in Kampung Melangkap along the Panataran River

2.2. Braiding Index Tool

In this study, the tool developed by Das and Islam [32] for estimating degree of braiding intensity is being used. This tool consists of four braiding indices that cover important aspects of braided rivers.

The first index of Das and Islam’s braiding index tool is the ratio of the area occupied by bars (A_b) to the area occupied by the reach (A_r), which is denoted by the BI^* :

$$BI^* = \frac{\sum A_b}{A_r} \quad (1)$$

The second index of the tool (i.e. BI_1), is taking into account the number of bars (N_b):

$$BI_1 = 1 - \frac{1}{\sum N_b} \quad (2)$$

Following a heavy consideration of this index on the bar parameters (“no bars, no braids”), the third index, i.e. BI_2 , showcases the intensity of the braiding influenced by the area and number of bars:

$$BI_2 = \left(\frac{\sum A_b}{A_r} \right) \times \left(1 - \frac{1}{\sum N_b} \right) \quad (3)$$

Finally, the braiding intensity (i.e. BI_3) is manifested with the bar parameters (areas and numbers) combined with the ratio of the lengths of channels in the reach:

$$BI_3 = \left[1 - \frac{L_{cmax}}{L_{ctot}} \right] \times \left(\frac{\sum A_b}{A_r} \right) \times \left[1 - \frac{1}{\sum N_b} \right] \quad (4)$$

where L_{cmax} is mid-channel length of the widest channel through the reach section, and L_{tot} is the sum of mid-channel lengths of all the segments of primary (widest) channel in the reach section.

This braiding index is unit-free, and the values have known limits which are 0 (no braiding, no bars) to 1 (unity, 100% braiding). To apply this braiding index tool, these rules were followed:

- (a) Only mid-channel bars or bars surrounded by wetted channels are considered. In this study, the bars were digitised from satellite images.
- (b) The length of reach section is $10w$, where w = width of the channel.

2.3. Collation of Satellite Images and Discharge Data

To analyse the braiding indices for the Panataran river, the riverbanks and the mid-channel bars were extracted from the satellite images obtained from the Google Earth Pro software application, version 7.3. High-resolution satellite images of the rivers were acquired for the year 2014 and 2016, representing the pre-seismic and post-seismic debris flow conditions respectively. The details of the acquired satellite images are presented in Table 1. Using the satellite image of the pre-seismic debris flow condition in 2014, the Panataran river is divided into 6 reach sections, ensuring that each section length is equivalent to $10w$ as required by Das and Islam [32] braiding index tool in Sec. 2.2. The same 6 reach sections are applied on the satellite image of the post-seismic debris flow condition in 2016 for the ease of the comparative

analyses between both debris flow conditions. Then, the riverbanks and mid-channel bars are digitised for both images, which are illustrated in Figure 3.

Table 1. Details of Google Earth satellite images of the Panataran River used in the study

Acquisition Date	Satellite Image Provider	Discharge (m ³ /s)	Status
1 st November 2014	CNES/Airbus	30.59	Pre-debris flow
19 th January 2016	CNES/Airbus	33.45	Post-debris flow

In addition to the satellite data, daily river discharges data from Tamu Darat Agricultural Station (Station ID: 1340031SF) were obtained from the Sabah State Department of Irrigation and Drainage, Malaysia for the acquisition dates of the satellite images (Table 1), i.e. 1st November 2014 and 19th January 2016. It is worth noting that the Tamu Darat gauging station also provides sediment discharge records, however the gauging equipment was damaged due to the debris flow event thus is not collated for this study. The river discharge data is obtained to determine the flow conditions in the main river for each period. It is found that the river discharges on 1st November 2014 and on 19th January 2016, which are about 7 months before and 7 months after the 2015 debris flow event respectively, are very similar with only a small difference of 3%. The close similarity of the pre- and post-debris flow discharges validates the suitability of using these two satellite images to further assess the impacts of the debris flow event on the braided patterns of the Panataran river.

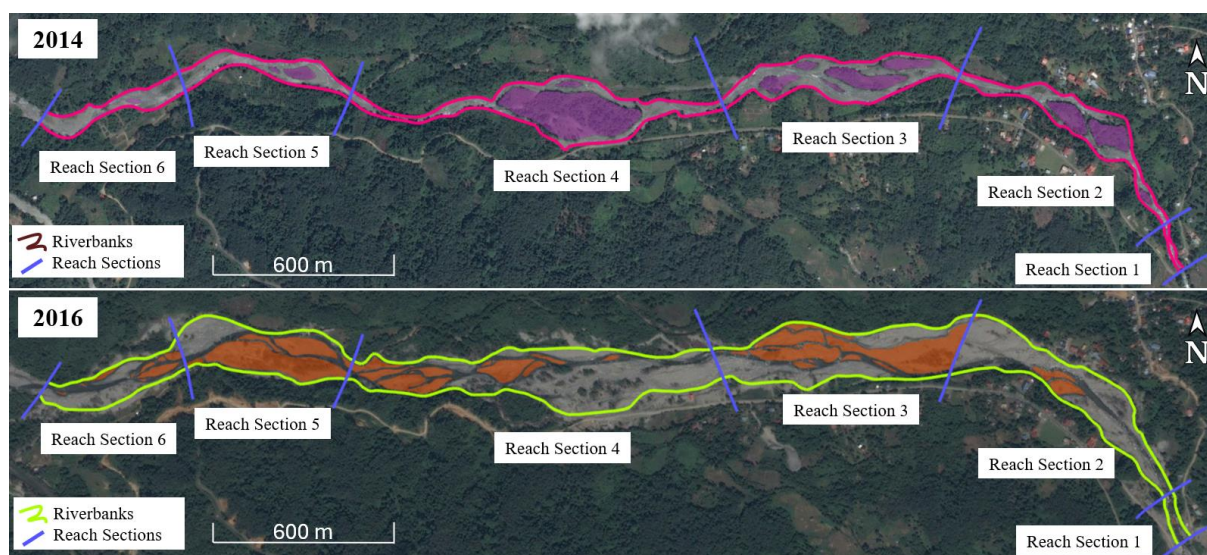


Figure 3. Satellite images of Panataran River with its banks, reach sections and mid-channel bars in the year 2014 (top panel) and in 2016 (bottom panel)

3. Results and Discussions

Figure 4 presents the values of the braiding indices BI^* , BI_1 , BI_2 and BI_3 plotted against six reach sections of the Panataran River (Figure 3) for both the pre-seismic debris flow condition (i.e. 2014), represented by the solid blue lines, and the post-seismic debris flow condition (i.e. 2016), represented by the solid red lines. The BI^* values plotted against the reach sections (Figure 4(a)) indicated that the mid-channel bar areas in section 1 have shown a very small increase after the debris flow event. This change may be attributed to the section's proximity to the bailey bridge (Figure 1), which could have constricted the debris flow upstream. As a result, higher-velocity flows would have prevented the deposition of bed and suspended sediment loads in section 1. The effects of high-velocity flows from the bailey bridge are more evident in section 2, which shows lower BI^* in 2016 compared to the 2014 pre-seismic debris flow condition of 2014. This suggests that the high kinetic energy from the debris flow eroded the bars, leading to a significant reduction in bar areas. In contrast, section 3 experienced a substantial increase in BI^* in 2016. This increase can likely be attributed to the abrupt directional change of the river flow from northeast to east, which resulted in a slight reduction in flow velocity. This reduction induced the deposition of bed sediment close to the riverbanks and the accumulation of suspended sediment loads, which formed mid-channel bars in section 3. The BI^* value at section 4 is observed to be lower in 2016 than in 2014, albeit it is still considered higher compared to the BI^* value at section 2 in 2016. This suggests that the mid-channel bars in section 4, which were present in 2014 (see Figure 3, top panel), underwent significant erosion following the post-seismic debris flow event (see Figure 3, bottom panel). However, the river flow in section 4 appeared to have less kinetic energy, which may have allowed the eroded mid-channel bars coupled with the sediment loads carried by the debris flow to disperse downstream into multiple, smaller mid-channel bars, resulting in a reduction in total bar area. The effects of the debris flow on bar areas are most pronounced in sections 5 and 6, where a noticeable increase in BI^* values is observed. This indicates that the slowing of the river flow in these sections after the debris flow event promoted the growth of the mid-channel bars and thus increased the total bar areas.

In Figure 4(b), which illustrates the BI_1 values plotted against the reach sections, the number of mid-channel bars in sections 1 and 2 experienced little to no change, or only a very small increase, following the post-seismic debris flow event in 2015. This suggests that the impact of the debris flow on the number of bar formation in these upstream sections was relatively limited, with sediment dynamics possibly being influenced by factors such as flow velocity or sediment supply, which may have prevented significant bar development. Notable increase in the BI_1 values is observed beyond section 2, i.e. sections 3–6. This indicates that the mid-channel bars in these downstream

sections experienced more substantial changes following the debris flow event. The largest increase in BI_1 values occurred in section 6, which is the most downstream reach section of the Panataran river. This section saw the most pronounced growth in the number of bars, suggesting that the debris flow event led to more extensive bar formation. The observed rise in mid-channel bar numbers in section 6 corresponds closely with the earlier discussed increase in bar areas (as indicated by BI^*), supporting the statement that sediment deposition and mid-channel bar growth were significantly enhanced in this downstream reach sections.

The BI_2 values plotted against the reach sections in Figure 4(c) reveal that the trends resulted from the combined influence of the bar parameters, i.e. BI^* and BI_1 , in sections 1 to 6 in 2016 closely mirrored the trends observed in the bar areas (i.e. BI^*) in the same area as shown in Figure 4(a). In particular, sections 1, 2 and 4 exhibited a reduction in BI_2 , whereas sections 3, 5 and 6 showed the opposite trend, with an increase in BI_2 . These observations also implied that the combined influence of the bar parameters (i.e. BI_2) is more strongly influenced by the bar areas (i.e. BI^*) rather than by the number of bars (i.e. BI_1) in the reach sections of the Panataran river. This suggests that the size of the bar area is a key factor driving changes in the BI_2 values, and that changes in the number of bars alone do not necessarily correlate with significant shifts in river morphology or define the braided patterns of the Panataran river.

The BI_3 values, which represent the braided intensity of a reach section resulting from the combined effects of bar parameters (i.e. BI_2) and the reach's channel length, are plotted against the reach sections in Figure 4(d). The trends in the BI_3 values across the six sections are similar to those of the BI_2 values. However, there is a slight decrease in the BI_3 values compared to the BI_2 values at section 5. This suggests that braiding intensity is strongly influenced by the total length of the channel surrounding the mid-channel bars and is indirectly dependent on the number of existing mid-channel bars in the reach section. These observations indicate that BI_3 is primarily influenced by BI_2 , and in particular by BI^* (as earlier discussed in the BI_2 trends), in sections with low numbers of mid-channel bars. However, in sections with a large number of mid-channel bars, the total length of the channel, or by proxy, the number of bars (BI_1), may also play a role in determining braiding intensity in the reach sections of the Panataran river.

Table 2 presents the differences in braiding index values between the post-seismic debris flow condition in 2016 and the pre-seismic debris flow condition in 2014 across six reach sections. Based on this table, section 5 stands out in most of the braiding indices. The significant increase in BI^* suggests increment in sediment deposition which formed more bars within the river channel, which in turn influenced both BI_2 and BI_3 (i.e. braiding intensity). This likely reflects changes in the sediment transport and flow dynamics in this reach section, particularly the substantial

deposition of bedload sediment and possibly a shift in braided river morphology following the post-seismic debris flow event. Section 6 shows the highest increase in BI_1 , indicating the greatest concentration of mid-channel bars throughout the Panataran river. This suggests that sediment deposition is most pronounced in this section, possibly due to reduced flow velocity. Despite this, section 6 still exhibits smaller total bar area compared to section 5, which implies that although there a greater number of bars in section 6, each bar is smaller in size. In contrast, section 2 experienced significant reductions across most of the braiding indices, indicating considerable river erosion. This suggests that section 2 is less conducive to mid-channel bar

formation and shows fewer braided patterns, likely due to a combination of erosional forces and flow changes post-debris flow.

The comprehensive braiding index tool developed by Das and Islam [32] has proven effective in highlighting the sections of the Panataran river that are most affected by the post-seismic debris flow event in 2015. These findings on sediment transport and river patterns, as quantified by the Das and Islam’s braiding indices, not only deepen our understanding of fluvial dynamics, bar formation and river erosion in post-seismic environments but also serve as valuable inputs for sustainable ecotourism planning and flood risk assessment in seismic regions.

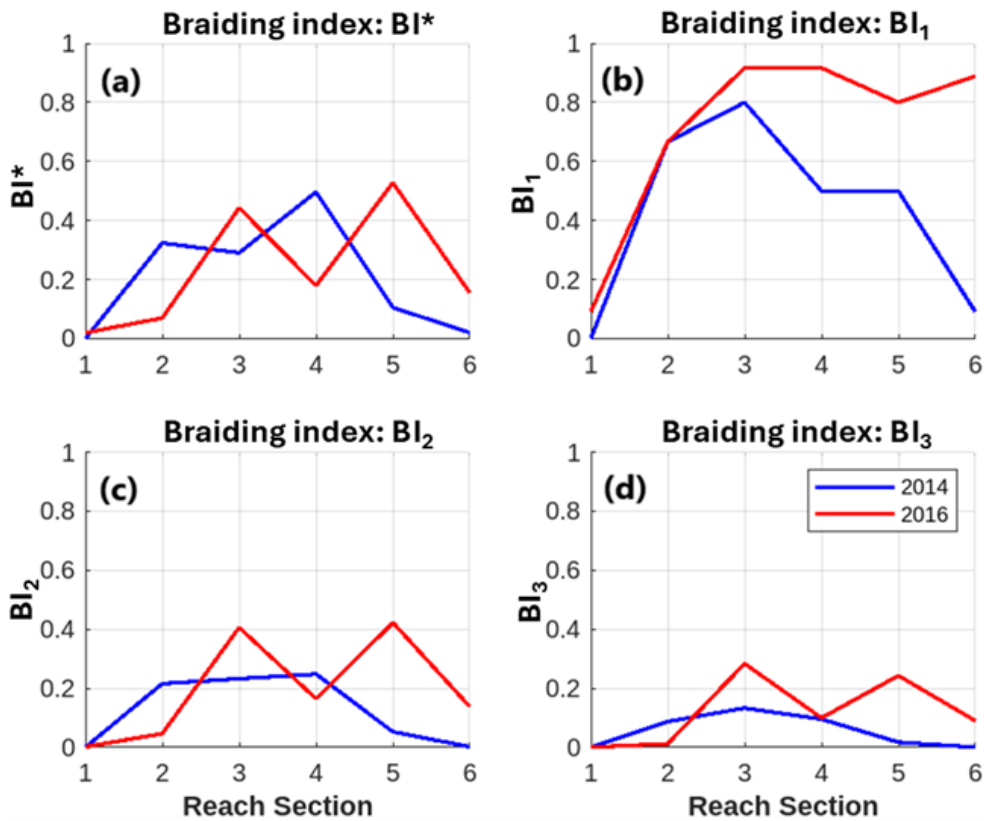


Figure 4. The values of the braiding indices at 6 reach sections of the Panataran river: (a) BI^* relating to the bar area; (b) BI_1 relating to the numbers of bars; (c) BI_2 relating to the influence of bar parameters to the braiding intensity; and (d) BI_3 relating to the influence of the bar parameters and the channel length to the braiding intensity in the reach sections

Table 2. Difference of braiding index values between the post-debris flow event (2016) and pre-debris flow event (2014) across 6 reach sections

Braiding index	Reach sections					
	1	2	3	4	5	6
BI^*	1.99E-02	-25.4E-02	15.2E-02	-31.7E-02	42.3E-02	13.4E-02
BI_1	9.09E-02	No change	11.7E-02	41.7E-02	30.0E-02	79.8E-02
BI_2	0.18E-02	-16.9E-02	17.3E-02	-8.4E-02	37.0E-02	8.50E-02
BI_3	0.05E-02	-7.49E-02	15.0E-02	0.42E-02	22.6E-02	8.98E-02

4. Conclusions

This study demonstrates the practical adaptability of the Das & Islam [32] braiding index tool in assessing sediment dynamics in post-seismic environments, revealing the tool's capacity to detect nuanced morphological changes in braided rivers. By applying this tool to the Panataran river, this study contributes a structured approach to understanding how post-seismic debris flow events influence complex fluvial systems, particularly in sediment-laden braided rivers. These insights are crucial for advancing riverine geomorphological assessments in seismic regions and promoting improved riparian management strategies. Beyond its immediate applications, this study highlights the importance of integrating quantitative tools in post-disaster studies, encouraging future work to expand such indices to diverse river settings impacted by natural disasters such as floods and debris flows. Ultimately, this tool offers a valuable resource to policymakers and environmental managers in making informed, data-driven decisions for both risk mitigation and sustainable development in vulnerable riverine landscapes.

Acknowledgements

This study is financially supported by the Universiti Malaysia Sabah Research Cluster Fund No. DKP0039. We are very grateful to Kenneth Chung for providing the aerial photo of the eco-tourism industries in the Panataran river, and the reviewers for their appropriate and constructive suggestions to improve this manuscript.

REFERENCES

- [1] B. Lehner, C.R. Liermann, C. Revenga, C. Vörösmarty, B. Fekete, P. Crouzet, P. Döll, M. Endejan, K. Frenken, J. Magome, and C. Nilsson, "High-resolution mapping of the world's reservoirs and dams for sustainable river-flow management," *Frontiers in Ecology and the Environment*, vol. 9, no. 9, pp. 494–502, Nov. 2011, DOI: 10.1890/100125.
- [2] C.-W. Chang, P.-S. Lin, and C.-L. Tsai, "Estimation of sediment volume of debris flow caused by extreme rainfall in Taiwan," *Engineering Geology*, vol. 123, no. 1, pp. 83–90, 2011, DOI: 10.1016/j.enggeo.2011.07.004.
- [3] S. He, D. Wang, S. Chang, Y. Fang, and H. Lan, "Effects of the morphology of sediment-transporting channels on the erosion and deposition of debris flows," *Environmental Earth Sciences*, vol. 77, no. 14, pp. 1–13, Jul. 2018, DOI: 10.1007/s12665-018-7721-y.
- [4] E. Kusratmoko, A. Wibowo, and A. Ahmad Kurnia, "Changes in the Value of Sinuosity Index in Komering River Channel, Province South Sumatera Years 1990 - 2016," in *IOP Conference Series: Earth and Environmental Science*, Institute of Physics Publishing, Nov. 2019. DOI: 10.1088/1755-1315/338/1/012024.
- [5] A. Suresh, A. Chanda, Z.A. Rahaman, A.A., Kafy, S.N. Rahaman, M.I. Hossain, M.T. Rahman, and G. Yadav, "A geospatial approach in modelling the morphometric characteristics and course of Brahmaputra river using sinuosity index," *Environmental and Sustainability Indicators*, vol. 15, Sep. 2022, DOI: 10.1016/j.indic.2022.100196.
- [6] A. Khan, L. A. K. Rao, A. P. Yunus, and H. Govil, "Characterization of channel planform features and sinuosity indices in parts of Yamuna River flood plain using remote sensing and GIS techniques," *Arabian Journal of Geosciences*, vol. 11, no. 17, Sep. 2018, DOI: 10.1007/s12517-018-3876-9.
- [7] H. Hazarika, D. Rohit, S.M. Pasha, T. Maeda, I. Masyhur, A. Arsyad, and S. Nurdin, "Large distance flow-slide at Jono-Oge due to the 2018 Sulawesi Earthquake, Indonesia," *Soils and Foundations*, vol. 61, no. 1, pp. 239–255, Feb. 2021, DOI: 10.1016/j.sandf.2020.10.007.
- [8] F. Bari, B. Istijono, R. Yuhendra, A. Hakam, M. Noer, and T. Ophiyandri, "Potential debris flow after earthquake in Mount Talamau Pasaman district and West Pasaman district," in *IOP Conference Series: Earth and Environmental Science*, Institute of Physics, 2023. DOI: 10.1088/1755-1315/1173/1/012069.
- [9] S. Ghosh and B. Mistri, "Hydrogeomorphic Significance of Sinuosity Index in relation to River Instability: A Case Study of Damodar River, West Bengal, India," *International Journal of Advances in Earth Sciences*, vol. 1, no. 2, pp. 49–57, 2012, DOI: 10.13140/2.1.4424.6089.
- [10] P. Nimnate, "Ancient and modern fluvial geomorphology of meandering system from upstream area of the Mun River, Changwat Nakhon Ratchasima," 2017.
- [11] D. Lalramchulloa, C. U. Bhaskra Rao, and P. Rinawma, "Morphometric and Sinuosity Analysis of Tlawng River Basin: A Geographic Information System Approach," *Journal of Geographical Studies*, vol. 5, no. 1, pp. 22–32, May 2021, DOI: 10.21523/gcj5.21050103.
- [12] M. G. Kleinhans, and J. H. van den Berg, "River channel and bar patterns explained and predicted by an empirical and a physics-based method," *Earth Surface Processes and Landforms*, vol. 36, no. 6, pp. 721–738, May 2011, DOI: 10.1002/esp.2090.
- [13] N. D. Gordon, T. A. McMahon, B. L. Finlayson, C. J. Gippel, and R. J. Nathan, "It's Sedimentary, Watson!" in *Stream Hydrology An Introduction for Ecologists*, Second Edition, John Wiley & Sons Ltd, 2004, pp. 182–185.
- [14] L. B. Leopold and M. Gordon Wolman, *River channel patterns: braided, meandering, and straight*. US Government Printing Office, 1957.
- [15] M.K. Kamarudin, M.E. Toriman, N. Abd Wahab, M.A. Samah, K.N. Maulud, F.M. Hamzah, A.S. Saudi, and S. Sunardi, "Hydrological and climate impacts on river characteristics of pahang river basin, Malaysia," *Heliyon*, vol. 9, no. 11, Nov. 2023, DOI: 10.1016/j.heliyon.2023.e21573.
- [16] H. Piégay, G. Grant, F. Nakamura, and N. Trustrum, "Braided river management: from assessment of river

- behaviour to improved sustainable development,” in *Braided Rivers: Process, Deposits, Ecology and Management*, vol. 36, Blackwell Publishing Ltd, 2006, pp. 257–275.
- [17] B. S. Caruso, C. Pithie, and L. Edmondson, “Invasive riparian vegetation response to flow regimes and flood pulses in a braided river floodplain,” *Journal of Environmental Management*, vol. 125, pp. 156–168, 2013, DOI: 10.1016/j.jenvman.2013.03.054.
- [18] Z. Li, H. Lu, P. Gao, Y. You, and X. Hu, “Characterizing braided rivers in two nested watersheds in the Source Region of the Yangtze River on the Qinghai-Tibet Plateau,” *Geomorphology*, vol. 351, p. 106945, Feb. 2020, DOI: 10.1016/J.GEOMORPH.2019.106945.
- [19] K. Tockner, A. Paetzold, U. Karaus, C. Claret, and J. Zettel, “Ecology of Braided Rivers,” in *Braided Rivers: Process, Deposits, Ecology and Management*, vol. 36, Blackwell Publishing Ltd, 2006, pp. 339–359.
- [20] E. M. Latrubesse and T. M. Suizu, “The Geomorphology of River Wetlands,” *Encyclopedia of Inland Waters*, Second Edition, vol. 3, pp. 33–50, Jan. 2022, DOI: 10.1016/B978-0-12-819166-8.00209-7.
- [21] A. Mamun and M. Sobnam, “Dynamics of Dharla River in Bangladesh Relation to Sinuosity and Braiding: GIS-RS Based Spatial Investigation,” *IOSR Journal of Applied Geology and Geophysics*, vol. 9, no. 4, pp. 50–56, 2021, DOI: 10.9790/0990-0904025056.
- [22] M. P. Akhtar, N. Sharma, and C. S. P. Ojha, “Braiding process and bank erosion in the Brahmaputra River”, *International Journal of Sediment Research*, vol. 26, no. 4, pp. 431–444, Dec. 2011, DOI: 10.1016/S1001-6279(12)6003-1.
- [23] M. Hoseinzadeh, and A. Golestani, “Investigating changes in the braided pattern of the Jajroud River based on Brice, Richards and Warburton braiding indices (between Latian Dam and Mamlo Dam)”, *Quantitative Geomorphological Research*, vol. 12, no. 1, pp. 132–151, 2023, DOI: 10.22034/gmpj.2023.3675 66.1385.
- [24] M. B. Rashid, “Channel bar development and bankline migration of the Lower Padma River of Bangladesh”, *Arabian Journal of Geosciences*, vol. 13, no. 14, Jul. 2020, DOI: 10.1007/s12517-020-05628-9.
- [25] A. H. Nama, A. S. Abbas, and J. S. Maatooq, “Field and Satellite Images-Based Investigation of Rivers Morphological Aspects,” *Civil Engineering Journal (Iran)*, vol. 8, no. 7, pp. 1339–1357, Jul. 2022, DOI: 10.28991/CEJ-2022-08-07-03.
- [26] J. C. Brice, *Channel patterns and terraces of the Loup Rivers in Nebraska*. US Government Printing Office, 1964.
- [27] D. Germanoski and S. A. Schumm, “Changes in braided river morphology resulting from aggradation and degradation,” *Journal of Geology*, vol. 101, no. 4, pp. 451–466, 1993, DOI: 10.1086/648239.
- [28] P. F. Friend and R. Sinha, “Braiding and meandering parameters,” in *Braided Rivers*, vol. 75, Geological Society, 1993, pp. 105–111.
- [29] B. R. Rust, “A classification of alluvial channel systems,” in *Fluvial Sedimentology*, CSPG Special Publications, 1977, pp. 187–198.
- [30] A. D. Howard, M. E. Keetch, and C. L. Vincent, “Topological and geometrical properties of braided streams,” *Water Resources Research*, vol. 6, no. 6, pp. 1674–1688, 1970, DOI: 10.1029/WR006i006 p01674.
- [31] L. B. Hong and T. R. H. Davies, “A study of stream braiding,” *Geological Society of America Bulletin*, vol. 90, no. 12_Part_II, pp. 1839–1859, 1979, DOI: 10.1130/0016-7606(1979)90%3C1094:SOSBS%3E2.0.CO;2.
- [32] B. C. Das and A. Islam, “Reviewing braiding indices of the river channel in an attempt to establish alternatives,” *MethodsX*, vol. 10, p. 102042, 2023, DOI: 10.1016/j.mex.2023.102042.
- [33] A. Yadav, R. J. Boothroyd, G. H. Sambrook Smith, and S. Sen, “Morphological adjustments of the Yamuna River in the Himalayan foothills in response to natural and anthropogenic stresses,” *Hydrological Processes*, vol. 37, no. 7, Jul. 2023, DOI: 10.1002/hyp.14934.
- [34] B. Delcaillau, F. Graveleau, G. Rao, M. Le Bón, and D. Delcaillau, “Fluvial styles during fold growth: An example from the eastern segment of the Qiulitage and Yakeng folds, southern Tian Shan, China,” *Geomorphology*, vol. 443, p. 108933, 2023, DOI: 10.1016/j.geomorph.2023.108933.
- [35] K. Ghosh, T. Chakraborty, and P. P. Patel, “A new braiding index to assess river regulation effects in multi-thread channels: Insights from a highly regulated Himalayan river,” *River Research and Applications*, 2024, DOI: 10.1002/rra.4261.
- [36] U. K. Kamlun, C. F. Miuse, D. D. Puma, M. Mahali, W. Wong, and M. H. Phua, “Mapping pre and post earthquake land cover change in Melangkap, Kota Belud Sabah using multi-temporal satellite Landsat 8/OLI and Sentinel 2 Imagery,” in *IOP Conference Series: Earth and Environmental Science*, Institute of Physics, 2022. DOI: 10.1088/1755-1315/1053/1/012024.
- [37] L. T. Chai, A. Nainar, R. Roslee, W. V. C. Wong, and M. H. Phua, “Assessment of immediate and five-year earthquake impacts on river systems in Sabah, Malaysia using multi-temporal satellite imageries,” *Geoenvironmental Disasters*, vol. 11, no. 1, Dec. 2024, DOI: 10.1186/s40677-024-00276-7.
- [38] C. Payus, S. I. Anuar, B. Musta, K. Bidin, F. Tongkul, and P. Y. Moh, “Water Quality for River Basins after Post Earthquake Event,” *Environment and Ecology Research*, vol. 11, no. 1, pp. 218–223, Feb. 2023, DOI: 10.13189/eer.2023.110116.
- [39] F. Tongkul, *Earthquake Science in Malaysia: Status, Challenges and Way Forward*. Universiti Malaysia Sabah Press, <http://www.ums.edu.my> (accessed Sept. 11, 2024)
- [40] K. Sharir, G. T. Lai, N. Simon, L. K. Ern, E. Madran, and R. Roslee, “Debris flow susceptibility analysis using a bivariate statistical analysis in the Panataran River, Kg Melangkap, Sabah, Malaysia,” in *IOP Conference Series: Earth and Environmental Science*, Institute of Physics, 2022. DOI: 10.1088/1755-1315/1103/1/012038.
- [41] M.I. Rosli, F. Che Ros, K.A. Razak, S. Ambran, S.A. Kamaruddin, A. Nor Anuar, A. Marto, T. Tobita, and Y. Ono, “Modelling debris flow runout: A case study on the Mesilau Watershed, Kundasang, Sabah,” *Water*

(Switzerland), vol. 13, no. 19, Oct. 2021, DOI: 10.3390/w13192667.

Sustainability (Switzerland), vol. 14, no. 23, Dec. 2022, DOI: 10.3390/su142315832.

- [42] A. Jafar, R. Dollah, N. Sakke, M.T. Mapa, E.P. Joko, M.M. Radzi, U. Imang, S.A. Ahmad, A. Ab. Wahab, and J.A. Sipatau, "Tourism and Natural Hazards: River Landform Changes Due to Geohazards and Its Influence on the Economic Development of Ecotourism in Sabah, Malaysia,"
- [43] E. Gomes, "Firefighters rescue 25 trapped by flooding at Kota Belud campsite," The Borneo Post, <https://www.theborneopost.com/2022/12/23/firefighters-rescue-25-trapped-by-flooding-at-kota-belud-campsite/> (accessed Nov. 7, 2024)